ORGANOMETALLICS

Article

pubs.acs.org/Organometallics

Ru(II)-Triphos Catalyzed Amination of Alcohols with Ammonia via Ionic Species

Eric J. Derrah,[†,‡] Matthias Hanauer,[§] Philipp N. Plessow,[†,§] Mathias Schelwies,[‡] Marion K. da Silva,[‡] and Thomas Schaub*[,†,‡]

[†]CaRLa – Catalysis Research Laboratory, Im Neuenheimer Feld 584, D-69120 Heidelberg, Germany

[‡]Synthesis & Homogeneous Catalysis, and [§]Quantum Chemistry BASF SE, Carl-Bosch-Straße 38, D-67056 Ludwigshafen, Germany

Supporting Information

ABSTRACT: An active and selective system for the amination of primary alcohols to primary amines with ammonia based on ruthenium and triphos as the tridentate phosphine ligand was developed. On the basis of detailed mechanistic studies, we propose that the active catalyst is, unlike the previously reported systems on this reaction, a cationic ruthenium complex. The experimental findings are supported by detailed density functional theory (DFT) calculations on the catalytic cycle. Because of the cationic nature of the active catalyst, strong anion and solvent effects were observed in the catalytic amination reaction when using the ruthenium triphos complexes. Therefore, a higher activity could be achieved when the nonpolar solvent toluene is used in this amination instead of tetrahydrofuran. Our findings can help to develop and optimize the system systematically for an application to relevant target molecules.

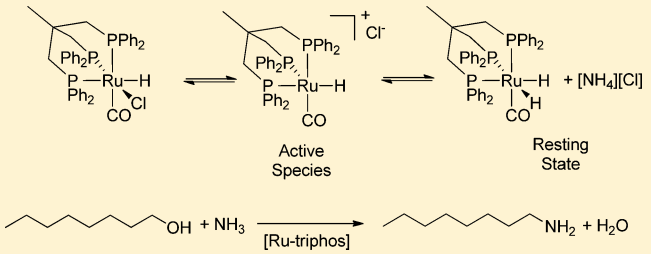

INTRODUCTION

Terminal primary amines are important industrial products and are used as synthons in fine chemical and pharmaceutical production. The transition metal catalyzed N-alkylation of ammonia with alcohols is an attractive method for amine formation due to its use of inexpensive and abundant starting materials, high atom economy, and water being the only side-product. Industrially, these amines are prepared by heterogeneous processes, but primary amine selectivity and substrate scope remain limited.[1] In order to overcome these drawbacks of the heterogeneous systems, a range of homogeneous catalysts have been developed in the last few years for selective alcohol amination.[2]

For different substrates, several ruthenium based catalyst systems could be identified for the desired amination of alcohols with ammonia. Among the most active are Milstein's acridine-based PNP-pincer Ru complex (**A**)[3] and the cyclohexyl derivate (**B**) from our laboratory,[4] Ru-CataCXiumPcy investigated by Beller et al.[5] as well as Vogt et al.,[6] Ru-Xantphos (**C**),[7] Ru-DPEphos,[8] and Ru-dppp or Ru-dppb (Figure 1).[8] Some of these catalysts were also successful in the amination of polyalcohols, which are quite challenging substrates for heterogeneous catalysts.[7,9]

Of the ruthenium based systems, only the Milstein type catalysts and the Xantphos system were studied in detail to gain mechanistic insight, which is fundamental to further development and optimization of the catalysts.[4,10,11]

A detailed mechanistic study of 1-octanol amination using **B** showed that the ligand's acridine backbone is protonated, inducing a coordination mode shift from meridional to facial.[4]

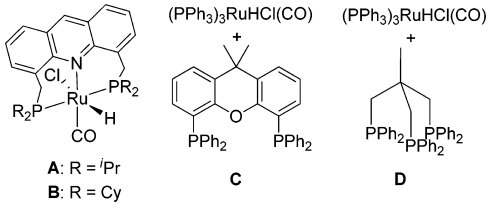

Figure 1. Ruthenium based homogeneous catalysts for the alcohol amination discussed in this work.

Furthermore, all species within the proposed catalytic cycle are neutral Ru-complexes with a tridentate coordination mode for this flexible ligand. In contrast, investigations by Vogt et al. imply that the potential tridentate Xantphos ligand is only coordinated to the ruthenium by the two phosphine substituents in all active species.[10] The crucial free coordination site is generated by PPh_3-dissociation, and only neutral Ru-species were proposed (Figure 2).

If the previously proposed mechanistic pathways based on **B** are suitable pathways for the Ru-catalyzed alcohol amination with NH_3, a more rigid tridentate ligand like triphos (1,1,1-tris(diphenylphosphinomethyl)ethane) could also generate an active catalyst. Despite the only moderate activity reported by Beller et al. using triphos in combination with $[Ru(acac)_3]$ or $[Ru_3CO_{12}]$ as catalyst for the alcohol amination,[7a] we tested triphos as a tridentate and stable phosphine ligand in

Received: January 2, 2015

DOI: 10.1021/acs.organomet.5b00003
Organometallics XXXX, XXX, XXX–XXX

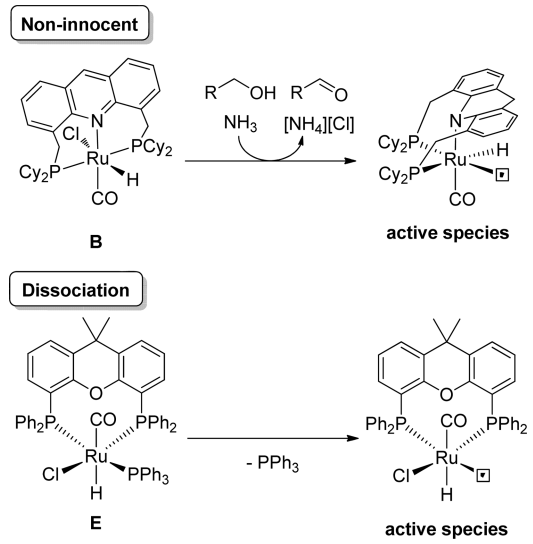

Figure 2. Active species formed through the noninnocent behavior of the acridine ligand in **B** (top)[4] or ligand dissociation from the Xantphos complex **E** (bottom).[10]

combination with our standard precursor [$(PPh_3)_3Ru(H)(Cl)(CO)$],[7b] in order to compare its amination activity directly with the acridine- or Xantphos-based catalysts.[3,4,7,11] When using this precursor with slightly more forcing conditions and higher catalyst loadings, we were able to generate an active and selective system for the synthesis of primary amines from alcohols and ammonia. In context of the previously mentioned work, the unexpectedly active triphos-based catalyst inspired a deeper mechanistic study, which is presented in this work.

RESULTS AND DISCUSSION

The triphos/[$(PPh_3)_3Ru(H)(Cl)(CO)$] (**D**) catalyst system was found to be active in the amination of 1-octanol with ammonia (Table 1). The conversion of 1-octanol (55%) and

Table 1. Amination of 1-Octanol with Ammonia Catalyzed by A–D[a]

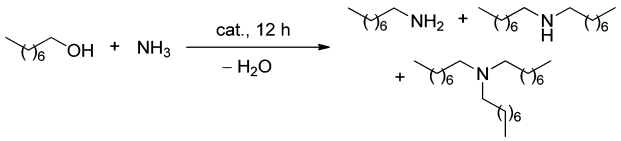

entry	cat.	T [°C]	conv. (%)	sel. (%)[b]
1	**A**	155	99	95
2	**B**	155	99	95
3	**C**	155	16	69
4	**D**	155	55	89
5	**D**[c]	155	26	81

[a][1-Octanol] = 1 M, 0.1 mol % catalyst, p(NH_3) = 35–40 bar, toluene (50 mL), 12 h, 160 mL stainless-steel autoclave. [b]Selectivity in 1-octylamine. [c]Tetrahydrofuran (THF) as solvent.

the selectivity for octylamine (89%) with **D** was lower than that with catalysts **A** and **B** under the standard catalytic conditions developed previously in our laboratory[4] but higher than that in the case of the Xantphos catalyst **C**. This preliminary result shows that **D** can serve as an alternative to the acridine based systems and is especially attractive due to the commercial availability of the common triphos ligand.

A strong solvent effect was observed for the reaction catalyzed by **D**. If THF was used instead of toluene (entry 5), the activity was significantly lower for **D**. Therefore, toluene was preferred as the solvent in most of the further investigations.

To gain first insight into potentially active species in the catalysis, we monitored the reaction via in situ IR spectroscopy. This is an ideal method to study this reaction as aldehyde, imine, and Ru-CO intermediates have unique stretching frequencies that are discernible. To limit the number of potential complexes in the reaction mixture and to rule out any influence of free PPh_3, the isolated complex [(triphos)Ru(H)(Cl)(CO)] (**1**, Scheme 1) was used instead of **D**.[12]

Scheme 1. Methods of Dihydride Complex 2 Formation

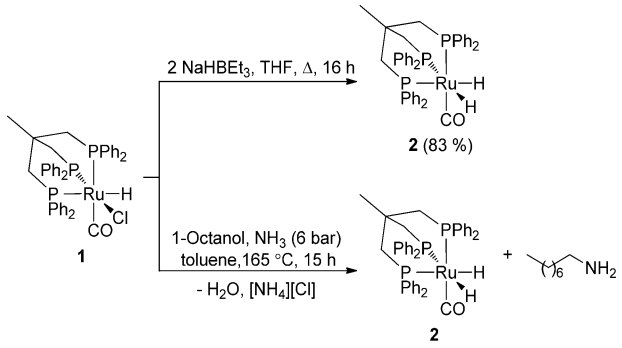

The amination of 1-octanol with ammonia was performed in a 20 mL ReactIR autoclave with a 7 mol % catalyst loading to match the detection limit of the apparatus. Toluene, complex **1**, and 1-octanol were added sequentially at 80 °C. The ν_{CO} = 1967 cm^{-1} of complex **1** is present until the addition of ammonia after which no carbonyl containing species are observed. As the temperature was slowly increased to 150 °C, a new ν_{CO} at 1934 cm^{-1} appears and is present for the remainder of the reaction (at 160 °C). Two other carbonyl stretches at 2066 and 1994 cm^{-1} are also observed, and no aldehyde (ν_{CO} = 1820–1670 cm^{-1}) or imine (ν_{CN} = 1690–1640 cm^{-1}) intermediates are present (Figure 3).[13]

The ν_{CO} (1934 cm^{-1}) of the main species is consistent with the known ruthenium dihydride complex [(triphos)Ru(H)$_2$(CO)] (**2**, ν_{CO} = 1934 cm^{-1} in DCM).[14] Independent

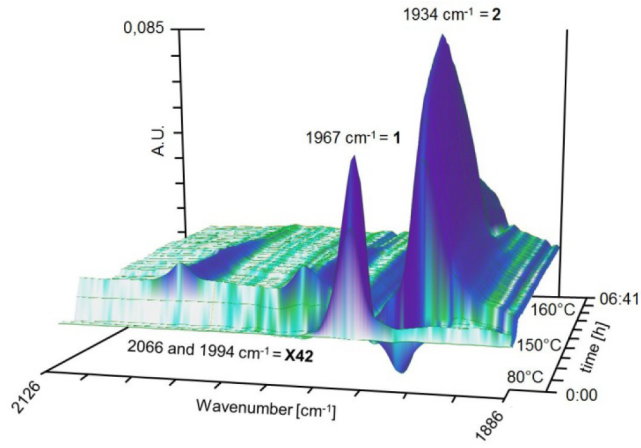

Figure 3. Portion of the *in situ* IR spectra of the 1-octanol amination reaction in toluene catalyzed by [(triphos)Ru(H)(Cl)(CO)] (**1**).

DOI: 10.1021/acs.organomet.5b00003
Organometallics XXXX, XXX, XXX–XXX

synthesis of **2** was achieved by the addition of [Na][$HBEt_3$] to **1** in refluxing THF (Scheme 1). All spectroscopic data are consistent with those reported in the literature and confirm accurate identification of **2**. Analysis of the crude amination reaction mixture shows that dihydride **2** is the sole ruthenium species at the end of catalysis. Therefore, based on the observations of the catalysis via react IR, **2** is likely the catalyst resting state.

Vogt et al. have shown in their detailed mechanistic study of cyclohexanol amination with ammonia, that the dihydride complex [(Xantphos)(PPh_3)Ru(H)$_2$(CO)] is the catalyst resting state and is formed directly from the alcohol.[10] This led us to the question, is **2** a catalytically active resting state that is accumulating, or is it a rather unreactive resting state? Consequently, we followed the catalytic amination of 1-octanol by GC with complexes **1** and **2** in THF at 155 °C over a 24 h period and compared it to **D** (Figure 4).

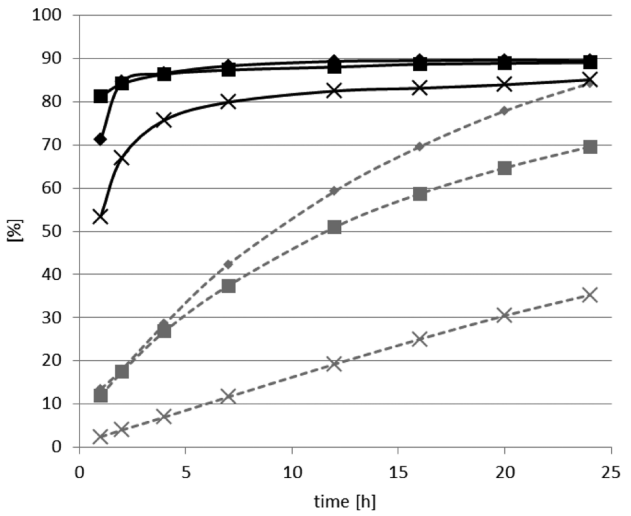

Figure 4. Reaction profile for 1-octanol amination with ammonia catalyzed by triphos/[(PPh_3)$_3$Ru(H)(Cl)(CO)] (**D**, ■), [(triphos)-Ru(H)(Cl)(CO)] (**1**, ♦), and [(triphos)Ru(H)$_2$(CO)] (**2**, ×). Selectivity (%) for the formation of octylamine is shown as solid black lines, and the conversion (%) of 1-octanol is shown as dashed gray lines. Conditions: 0.28 mol % catalyst, p(NH_3) = 35−40 bar, THF (30 mL), 155 °C, and 9.1 g of 1-octanol; reactions were carried out in a 160 mL stainless-steel autoclave.

Preformed catalyst **1** led to a higher conversion (84%) compared to **D**, with a similar selectivity for octylamine (90%). The higher rate of conversion indicates that excess PPh_3 slightly inhibits the reaction with **D**. The absence of an induction period when **D** was used shows that catalyst **1** is rapidly formed, which is further evidenced by a consistently high selectivity throughout the reaction. This is confirmed by the observation that no amination is observed if [(PPh_3)$_3$Ru(H)(Cl)(CO)] is used as the catalyst without triphos.

Dihydride complex **2** is the least active of the complexes tested (35% conversion after 24 h reaction time), but the selectivity (85%) was only slightly decreased. This points to the interpretation that if **2** is the catalyst resting state (Scheme 1) observed during the reaction by IR spectroscopy (Figure 3), then it is rather unreactive and must be converted to some extent into the active catalyst under the reaction conditions.

During catalysis, **2** is formed from **1** along with a stoichiometric amount of aldehyde and [NH_4][Cl]. Additionally, water is produced from the condensation reaction of octanal and ammonia. We thought that these reagents might influence the catalytic activity of **2**. In this context, excess octanal, [NH_4][Cl], and water (2.0 mol %) were added to the reaction catalyzed by **2** (0.2 mol %, toluene, 165 °C, 15 h). Surprisingly, the catalytic activity of **2** was restored, and selectivity and conversion similar to those of with **1** were achieved (Table 2). To determine which additive is most

Table 2. Additive Effects on the Amination of 1-Octanol with Ammonia Catalyzed by 1 or 2[a]

additive	conversion (%)	selectivity (%)[b]
	Catalyst **1**	
none	63	83
[NH_4][Cl]	67	80
octanal	89	90
	Catalyst **2**	
none	25	68
[NH_4][Cl], octanal, H_2O	61	85
[NH_4][Cl], octanal	87	69
[NH_4][Cl]	62	76
octanal, H_2O	0	0
octanal	0	0
acetone	0	0
cyclohexanone	0	0
acteophenone	0	0

[a]1-Octanol (3.6 mL), 0.2 mol % catalyst, 2.0 mol % additive, p(NH_3) = 6 bar, toluene (17 mL), 15 h, 60 mL stainless-steel autoclave. [b]Selectivity 1-octylamine.

important, one or more of the reagents was omitted in a systematic screening. When [NH_4][Cl] is present, the catalytic activity of **2** is significantly improved. No conversion of 1-octanol is observed when only water and/or 1-octanal were added (Table 2).

It is clear that [NH_4][Cl] is fundamental to the alcohol amination reaction catalyzed by **2**. To explore the role of ammonium, excess [NH_4][Cl] was added to a NMR tube containing **2** in pyridine-d_5. After 25 h at 110 °C, the sample contained monohydride **1** (83%) and a small amount of **2** (eq 1). With longer reaction times, the product began to

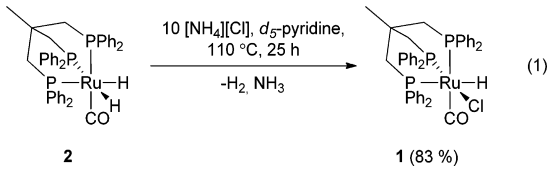

(1)

decompose. This indicates that [NH_4][Cl] protonates one Ru-H in **2**, regenerating **1** and stoichiometric amounts of H_2 and ammonia (low concentrations of H_2 precluded observance by NMR spectroscopy). This result indicates that dihydride **2** alone is likely outside of the productive catalytic cycle and that the combination of **2** with [NH_4][Cl] is the catalyst resting state.

If ammonium chloride is responsible for regenerating monohydride **1** from **2** with loss of hydrogen and ammonia, the principle of microscopic reversibility dictates that the reverse should be feasible. To this end, an autoclave containing **1** in THF was charged with ammonia (6 bar) and hydrogen (20 bar). After 1.5 h at 165 °C, the solution contained dihydride **2** (85%) with a small amount of unknown products (9%) and

DOI: 10.1021/acs.organomet.5b00003
Organometallics XXXX, XXX, XXX−XXX

unreacted **1** (6%). In the absence of ammonia, only 27% of **2** was present with an unknown product (6%, Scheme 2).

Scheme 2. Ammonia Facilitates Dihydride (2) Formation from 1 and H_2

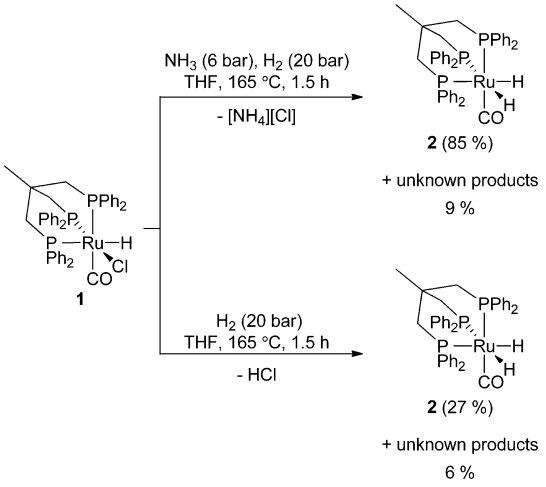

Addition of aldehyde improves the catalytic activity of **1**, although no activity was observed with **2**. Under standard catalytic conditions, only very small amounts of free aldehyde can be present. With the addition of excess octanal, the effective concentration of imine in solution is increased, giving a higher probability of imine hydrogenation by the active species. Experimentally, octanal (2.0 mol %) addition increased catalyst performance (89% conversion; 90% selectivity).

Ruthenium dihydride complex [(Xantphos)(PPh_3)Ru-$(H)_2$(CO)] (**F**) has been suggested by Vogt et al. to be the catalyst resting state in [(Xantphos)(PPh_3)Ru(H)(Cl)(CO)] (**E**) catalyzed amination of cyclohexanol by ammonia.[10] The dihydride is not catalytically active unless cyclohexanone (10 equiv) is added. This is logical since alcohol oxidation cannot occur directly from **F**. In our system, aldehyde addition only influences catalysis by monohydride **1**. No activity is observed with the addition of an aldehyde (octanal) or ketone (acetone, cyclohexanone, or acteophenone) to dihydride **2** (Table 2). In this instance, the catalytic activity of **2** is only restored in the presence of acidic [NH_4][Cl]. This suggests that a new mechanism of alcohol amination is needed to describe the catalytic activity with triphos complex **1**.

In order to gain a deeper understanding of the reaction mechanisms in place, a computational study was carried out. Electronic energies are obtained using the random phase approximation[15,16] (RPA) with PBE/def2-TZVPPD orbitals (using def2-TZVP for the C and H atoms on the triphos ligand and effective core potentials on Ru). Structures were optimized at the BP86/def2-SV(P) level of theory with the program package TURBOMOLE.[17] Computed free enthalpies include zero-point vibrational, and thermodynamic corrections (for T = 165 °C), as well as free enthalpies of solvation, were obtained from the COSMO-RS model (for a mixture of 74% toluene, 12% NH_3, and 5% each of 1-octanol, octylamine, and H_2O, and using a molar fraction of 0.02% for all other species) at the BP86/def2-TZVPD-fine level of theory with the program COSMOtherm.[18] The formation of solid [NH_4][Cl] was accounted for by the experimentally known free enthalpies of formation of [NH_4][Cl], NH_3, and HCl.[19,20] A more detailed discussion of the computational methodology and its accuracy may be found in the Supporting Information. Instead of 1-octanol, methanol is used as a model substrate in most calculations. For selected intermediates, values for ethanol as the substrate are provided in the schemes in parentheses.

We focused on mainly two distinct mechanistic proposals for the catalytic alcohol amination: the first one is analogous to the proposed mechanism of the acridine-based system as studied by Xe et al.[4,21] but involves a cationic active species because there is a third neutral phosphine side arm instead of a charged amide. The second proposal revolves around dihydride complex **2** as active species and mainly comprises neutral intermediates, analogous to Vogt's mechanistic proposal for the Xantphos-based system.[10,11] However, in the absence of a monodentate PPh_3 ligand, we consider the opening of one of the triphos ligand's side arms instead of a free dissociation of phosphine.

This neutral mechanism is reported in Scheme S1 of the Supporting Information and is unfeasible under the reaction conditions. Computed free activation enthalpies for side arm-opening of **2** trans to a hydride and trans to the carbonyl ligand are 162 and 167 kJ/mol, respectively. This is significantly higher than the estimated maximum barrier height ($\Delta G^{\ddagger}_{max}$ = 144 kJ/mol for 95% completion of a first-order reaction within 15 h at T = 165 °C) that can explain a slow reaction according to the Eyring equation. Even higher barriers result for the rate-determining transition state in the imine reduction ($\Delta G^{\ddagger}$ = 193 kJ/mol for ethanol as substrate). Therefore, a mechanism involving side arm dissociation may be safely dismissed.

Scheme 3 shows the proposed cationic mechanism. In agreement with the experimental observations, the active species **X1** forms from **2** through protonation by [NH_4][Cl] under the release of molecular hydrogen. Thus, the associated cost in free enthalpy (77 kJ/mol) depends on the partial pressure of hydrogen, which we set to a value roughly corresponding to the formation of H_2 through alcohol dehydrogenation in a yield of 3% (see the Supporting Information for details). The possibility to precipitate the chloride anion and to replace it by a better soluble noncoordinating counterion gives a handle to reduce this energy penalty and explains the observed speed-up when adding [Na][BAr^F_4] (see Figure 5). This activation step and the initial formation of aldehyde will be discussed below in detail (see also Scheme 5). For the present discussion, we assume the presence of a catalytic amount of aldehyde that is in equilibrium with the corresponding imine.

Similar to the mechanism in refs 4 and 21, imine reduction takes place after side-on coordination of imine by insertion into the Ru−H bond. Cleavage of the α-agostic interaction of the formed amide ligand is predicted to be the rate-determining step in the mechanistic cycle, with a barrier of $\Delta G^{\ddagger}$ = 139 kJ/mol (for ethanol as substrate), which is only slightly lower than the limiting value for a barrier that is still feasible under reaction conditions. In fact, cleavage of the agostic interaction and relaxation to the trigonal bipyramidal structure **X4** leads to a stabilization of about 40 kJ/mol. The Ru−N bond length reduces from 2.162 Å in **X3** to 1.975 Å in **X4**, which is in line with the formation of a Ru−N double bond. The incoming alcohol can then protonate the amide ligand and coordinate as an alkoxide to give the saturated cationic complex **X5**. After release of the amine, the alkoxide ligand in the trigonal bipyramidal complex **X6** undergoes oxidation to form a side-on bound aldehyde. This reaction sequence is the reverse of the imine reduction, however, with a lower barrier of $\Delta G^{\ddagger}$ = 113

DOI: 10.1021/acs.organomet.5b00003
Organometallics XXXX, XXX, XXX−XXX

Scheme 3. Proposed Cationic Mechanism for Catalytic Alcohol Amination[a]

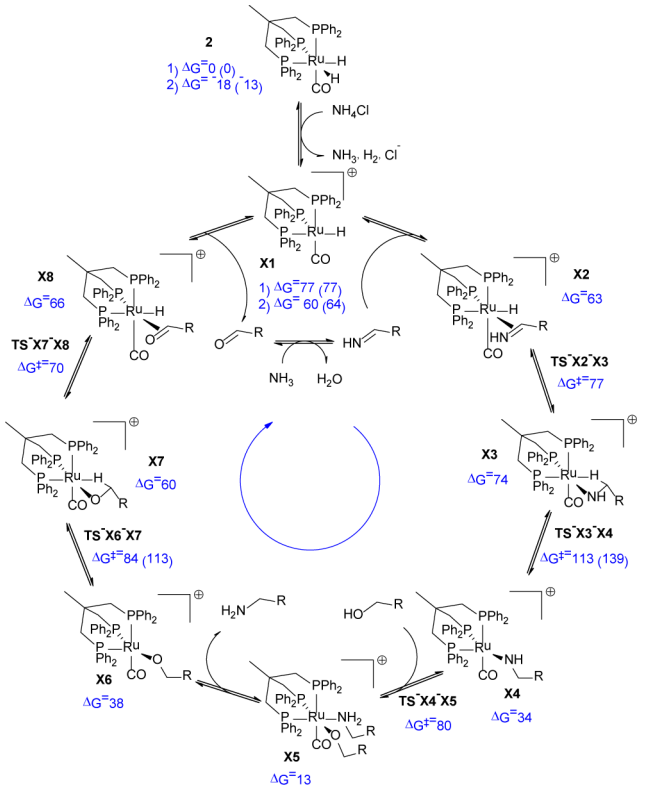

[a]Computed free enthalpies of reaction and activation are given in kJ/mol for R = H; values in parentheses correspond to R = Me. Values for 2 and X1 for the beginning of the cycle are numbered with 1 and with 2 for a complete cycle.

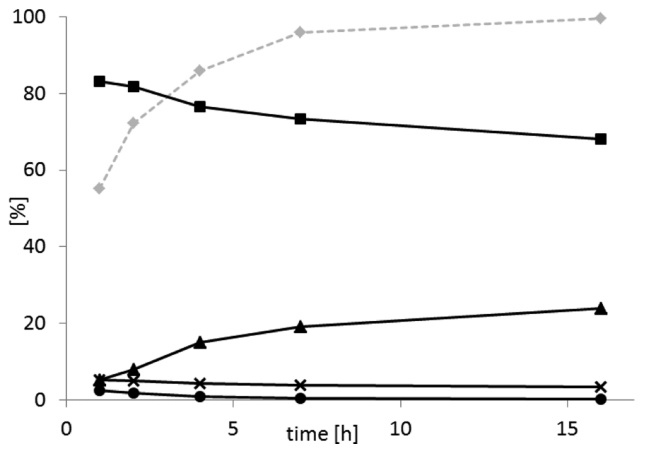

Figure 5. Reaction profile for 1-octanol amination with ammonia catalyzed by **1** (0.2 mol %) + [Na][Bar$^F_4$] (1.2 mol %), 6.5 g of 1-octanol, and 50 mL of toluene at 35−40 bar NH_3 and 155 °C; conversion (%) of 1-octanol is shown as a dashed gray line. Selectivity is shown as solid black lines for 1-octylamine (■), di-1-octylamine (▲), octanenitril (×), and octyl-octylidenamine (●).

kJ/mol (for ethanol). Dissociation of aldehyde closes the cycle, with a total gain in free enthalpy of $\Delta G = -13$ kJ/mol for the amination of ethanol ($\Delta G = -14$ kJ/mol for 1-octanol).

As an alternative pathway to the large barrier in the imine reduction step, Scheme 4 shows that breaking of the agostic interaction in **X3** may be assisted by protonation of the amide

Scheme 4. Alternative Pathway for the Rate-Determining Imine Reduction[a]

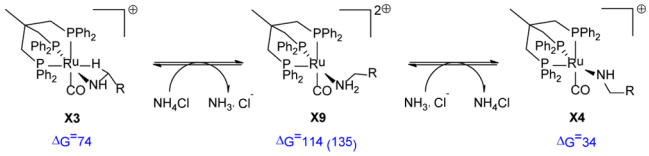

[a]Computed free enthalpies of reaction and activation are given in kJ/mol for R = H; the values in parentheses correspond to R = Me.

with excess $[NH_4][Cl]$. At the BP86/def2-SV(P) level of structure optimization, we have confirmed that the protonated form of **X3** relaxes to the dication **X9** and that the protonation and deprotonation reactions depicted in Scheme 4 are barrierless when using the $[NH_4]^+$ ion as an acid. Notably, the protonated form **X9** is a minimum on the BP86 energy surface. However, when accounting for the endergonic dissolution of solid $[NH_4][Cl]$, it becomes a maximum on the free enthalpy surface ($\Delta G = 135$ kJ/mol for ethylamine as ligand), which is energetically close to the highest transition state from Scheme 3. We note that the analogous step in the alcohol oxidation pathway is energetically unfeasible (see Scheme S2 in the Supporting Information).

Another alternative route leads to the formation of nitrile and is shown in Scheme S3 in the Supporting Information. Analogous to the mechanism proposed in refs 21 and 4, this pathway involves the coordination of imine to **X4**, followed by imine oxidation in a manner similar to the alcohol oxidation from Scheme 3. The release of side-on bound nitrile completes the reaction. The highest predicted barrier for the formation of acetonitrile is $\Delta G^‡ = 140$ kJ/mol, which is still feasible under reaction conditions and therefore in qualitative agreement with experimental observations (Figure 5).

Nitrile formation according to this mechanism is equivalent to a disproportionation of imine to amine and nitrile, and hence consumes two equivalents of aldehyde. The proposed cycle shown in Scheme 3, however, cannot explain the origination of aldehyde. In order to account for the formation of an excess amount of aldehyde and for the initial formation of dihydride complex **2** when using **1** as precatalyst, we propose that dehydrogenation of alcohol may take place as shown in Scheme 5: Starting from **1**, ligand substitution of alcohol for chloride leads to the cationic species **X11**. Dissociation of molecular hydrogen can take place after isomerization to **X13** with a barrier of $\Delta G^‡ = 148$ kJ/mol (for methanol as substrate). This isomerization may occur via either an internal protonation of the hydride ligand by the coordinated alcohol ($\Delta G^‡ = 151$ kJ/mol) or a subsequent deprotonation and protonation through **X12**, shuttled by ammonia. After liberation of hydrogen, the alkoxide complex **X6** can undergo the same alcohol oxidation mechanism mentioned above. Dihydride complex **2** could finally form from **X1** by barrierless addition of H_2 and subsequent deprotonation. An interesting alternative to the protonation of **X12** would in fact be the opening of the phosphine side arm trans to the carbonyl ligand, allowing the oxidation of the alcohol via the neutral mechanism shown in Scheme S1 (see Supporting Information) with a corresponding barrier of $\Delta G^‡ = 150$ kJ/mol ($\Delta G^‡ = 146$ kJ/mol for ethanol). This would directly yield catalytic amounts of aldehyde and dihydride complex **2**, while the formation of H_2 could occur afterward through the protonation of **2**.

DOI: 10.1021/acs.organomet.5b00003
Organometallics XXXX, XXX, XXX−XXX

Scheme 5. Proposed Mechanism for the Initial Formation of Aldehyde and Dihydride Complex 2[a]

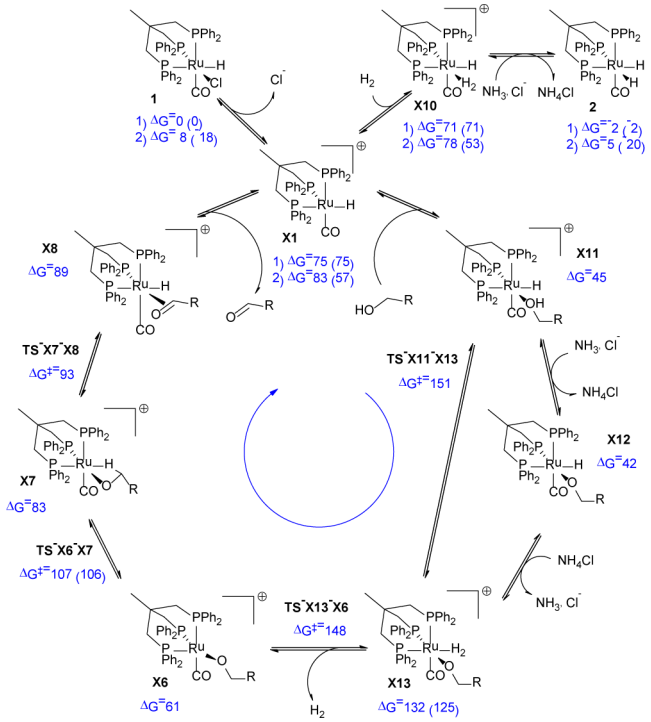

[a]Computed free enthalpies of reaction and activation are given in kJ/mol for R = H; the values in parentheses correspond to R = Me. The values for 1, 2, X1, and X10 for the beginning of the cycle are numbered with 1 and with 2 for a complete cycle.

Yet another possibility for the catalytic dehydrogenation of alcohol is shown in Scheme S4 of the Supporting Information. According to this scheme, protonation of the hydride ligand in **1** enables H_2 liberation with a barrier of $\Delta G^{\ddagger}$ = 141 kJ/mol and can thereby trigger alcohol oxidation, given that an initial amount of $[NH_4][Cl]$ is present.

A known side-reaction in Ru-catalyzed alcohol dehydrogenations is the decarbonylation of the alcohol, yielding Ru carbonyl complexes.[22] Starting from dihydride complex **2**, such decarbonylation reactions could lead to the formation of either dicarbonyl complex **X41** or the cationic dicarbonyl hydride complex **X42**, as shown in Scheme 6. Since these reactions are highly exergonic (ΔG < −100 kJ/mol), we also expect decarbonylation to occur as a side-reaction in the present system. Interestingly, Scheme 6 reveals that complexes **2** and **X42** are in an equilibrium with each other that depends on the pressures of CO and H_2 as well as the $[NH_4][Cl]/NH_3$ buffer. Indeed, the two carbonyl signals in the in situ IR spectrum occurring at 2066 and 1994 cm^{-1} agree reasonably well with literature values for **X42** measured in dichloromethane (2057 and 2010 cm^{-1}).[23] Therefore, we identify the observed species as $[(triphos)RuH(CO)_2]^+$ (**X42**). As X42 is considered to be a nonactive species in the catalysis, additional CO in the system presumably inhibits the catalysis due to an increased formation of **X42**. According to Scheme 6, a higher H_2 concentration in the system would decrease the concentration of **X42** but will also increase the amount of the resting state **2** (see Scheme 2).

Scheme 6. Possible Decarbonylation Reactions and Equilibrium between 2 and Dicarbonyl Hydride Complex X42[a]

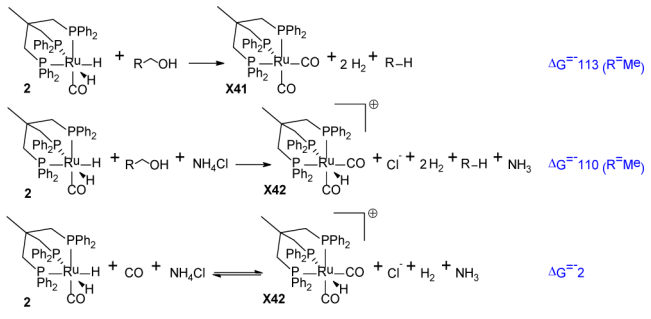

[a]Computed free enthalpies of reaction are given in kJ/mol for R = Me.

According to the proposed cationic mechanism for alcohol amination catalyzed by **1**, an increased concentration of a coordinating or badly soluble anion would decrease product formation. This is evidenced by greatly reduced 1-octanol conversion with excess NaCl and 18crown6 (2.0 mol %) addition (Table 3). Crown ether was needed to solubilize NaCl in the reaction medium. This further explains why excess $[NH_4][Cl]$ does not drastically increase 1-octanol conversion with **1** since any benefit from catalyst regeneration is eclipsed by increased chloride concentration (Table 2).

Table 3. Anion Effects on the Amination of 1-Octanol with Ammonia Catalyzed by 1[a]

anion source	conversion (%)	selectivity (%)[b]
none	63	83
NaCl, 18crown6[c]	37	84
$[Na][BAr^F_4]$	100	25

[a]1-Octanol (3.6 mL), 0.2 mol % catalyst, 1.2 mol % additive, p(NH_3) = 6 bar, toluene (17 mL), 15 h, 60 mL stainless-steel autoclave. [b]Selectivity 1-octylamine. [c]2.0 mol % anion source.

The poorly coordinating tetrakis[3,5-bis(trifluoromethyl)-phenyl]borate ($[BAr^F_4]^-$) greatly increased the catalytic activity of **1** for 1-octanol amination. However, the selectivity for octylamine was greatly reduced with dioctyl- and trioctylamine as major products when using the standard conditions. The reaction was monitored periodically over time (16 h) to get the full reaction profile (Figure 5), and a significantly higher NH_3 loading was used to decrease the di- and trialkylamine formation.

The activity of **1** increases significantly by adding 6 equiv of $[Na][BAr^F_4]$ when compared with that of the conversions given in Figure 4, where the same temperature and NH_3 amount were used. Conversions of over 80% and selectivities of about 80% to 1-octylamine could be observed even after 4 h, a finding that is consistent with the hypothesis that the active catalytic species is the cationic complex, stabilized in this case by the less coordinating $[BAr^F_4]$-anion. In contrast to the other catalyst used, the activity is high enough that also significant amounts of di-1-octylamine were obtained from the initially formed 1-octylamine. Therefore, it is important to stop the reaction early enough to achieve a high selectivity toward the desired 1-octylamine. The octanenitrile and octyl−octylideneamine byproducts are also initially formed with less than 3% selectivity. Their concentration decreases over time, so they can be considered as intermediates.

Anion effects could have significant impact on the amination reaction catalyzed by $[(triphos)Ru(H)_2(CO)]$ (**2**). This

DOI: 10.1021/acs.organomet.5b00003
Organometallics XXXX, XXX, XXX−XXX

manifests not only in anion coordination strength but also catalyst regeneration as a function of ammonium salt acidity. Ammonium salts or acids with coordinating anions are expected to have lower 1-octanol conversions. As expected, no conversion was observed with the addition of hydrogen cyanide (Table 4), presumably due to strong coordination of the anion at the ruthenium center of the active species (**X1**). Ammonium fluoride continued this trend giving significantly lower conversion (25%) with high selectivity (88%) relative to those of ammonium chloride. Surprisingly, bromide gave only slightly increased conversion (30%) with low selectivity (67%) compared to those of $[F]^-$, and no conversion was noted with ammonium iodide.

Table 4. Acidity and Anion Effects on the Amination of 1-Octanol with Ammonia Catalyzed by 2[a]

acid	pK_a	conv. (%)	sel. (%)[b]
none		25	68
HCN[c]	9.2	0	0
$[NH_4][F]$	−1.75 ± 0.7	25	88
$[NH_4][Cl]$	−1.03 ± 0.7	62	76
$[NH_4][Br]$	−1.03 ± 0.7	30	67
$[NH_4][I]$	0.31 ± 0.7	0	0
NaCl, 18crown6[d]		0	0

[a]1-Octanol (3.6 mL), 0.2 mol % catalyst, 2.0 mol % acid, $p(NH_3)$ = 6 bar, toluene (17 mL), 15 h, 60 mL stainless-steel autoclave. [b]Selectivity 1-octylamine. [c]Formed *in situ* by the thermolysis of cyanohydrin. [d]0.4 mol %.

The results from the acid and ammonium salt screening with catalyst **2** (see Table 4) do not appear to follow the expected trends, particularly in the case of $[NH_4][Br]$ and $[NH_4][I]$. The latter may be explained by poor solubility in the reaction media. The former, however, would be expected to give results comparable to or slightly better than those obtained with $[NH_4][Cl]$. Efficiency in regeneration of the active catalyst from **2** may explain the discrepancy. In an NMR tube reaction, $[NH_4][F]$ or $[NH_4][Br]$ were added to **2** in d_5-pyridine, and the solutions were heated at 110 °C (eq 2).

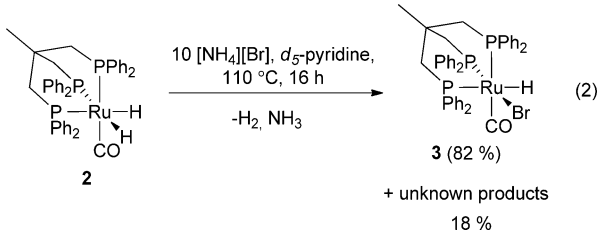

(2)

For the addition of $[NH_4][F]$ to **2**, no defined complex could clearly be characterized. Small amounts of what appears could be assigned by ^{31}P NMR to be [(triphos)Ru(H)(F)(CO)] or [(triphos)Ru(H)(CO)(Py)][HF_2] after 48 h besides a lot of unreacted **2**. Unfortunately, low concentration, even with extended reaction times, precludes complex characterization. Conversely, complete consumption of **2** was observed in 16 h with $[NH_4][Br]$. The monohydride [(triphos)Ru(H)(Br)(CO)] (**3**, 82%) was the main species, but a significant amount of decomposition was observed (18%, eq 2).

The strong coordination of F^- decreases the overall activity of the system, and also the low solubility of $[NH_4][F]$ is certainly playing a role. For $[NH_4][Br]$, conversion from **2** to the active catalyst (**3**) is relatively fast, but the complex is unstable. Therefore, the poor catalyst performance of $[NH_4][Br]$/**2** is a function of catalyst stability and not acidity, anion coordination, or solubility.

To ensure that the acid is responsible for the observed reactivity in these reactions and not solely the presence of an anion, nonacidic anion source (NaCl and 18crown6), was added to the amination reaction catalyzed by dihydride **2**. A lower salt concentration (0.4 mol %) was used to ensure that any catalyst activation was not suppressed by high chloride concentrations. Under these conditions, no catalytic activity was observed. This is consistent with our assumption that an acid is required to regenerate active species **1**. A similar behavior was reported by Leitner et al. on hydrogenations using ruthenium triphos catalysts.[24] They could also generate active species from the inactive complex **2** by the addition of an acid, whereby the general formation of cationic ruthenium complexes starting from neutral dihydrides is well-known.[25] In contrast to the observations made by Leitner et al.[24] and Cantat et al.,[26] the carbonyl ligand is still involved in the active species for the alcohol amination with NH_3 using these types of catalysts. Interestingly, the ammonia salts are acidic enough to generate the active species even under the basic conditions of the amination.

The testing of ammonium salts in this reaction shows that solubility is a critical factor on catalyst performance. This is predicted to be especially important for the [(triphos)Ru(H)(Cl)(CO)] (**1**) catalyzed reaction. During the reaction, water is generated as well as a stoichiometric amount of $[NH_4][Cl]$. As the water concentration increases, $[NH_4][Cl]$ could be drawn from the organic phase to the aqueous one. Therefore, crown ether (18crown6 2.0 mol %) was added to catalyst **1** to increase $[NH_4][Cl]$ solubility.[27] High conversion (88%) and selectivity (89%) for octylamine were observed. Higher conversion (96%) and comparable selectivity (88%) were further obtained with a combination of 18crown6 (2.0 mol %) and octanal (2.0 mol %, Table 5). Under these new conditions, higher conversion and selectivity can be obtained with **1** using comparable conditions.

Table 5. Crown Ether Effects on the Amination of 1-Octanol with Ammonia Catalyzed by 1[a]

anion source	conversion (%)	selectivity (%)[b]
none	63	84
18crown6	88	89
18crown6, octanal	96	88

[a]1-Octanol (3.6 mL), 0.2 mol % catalyst, 2.0 mol % additive, $p(NH_3)$ = 6 bar, toluene (17 mL), 15 h, 165 °C, 60 mL stainless-steel autoclave. [b]Selectivity 1-octylamine.

CONCLUSIONS

In contrast to the previously published mechanisms on the Ru-catalyzed alcohol amination using acridine-type ligands (**A**,**B**) or Xantphos (**C**), the active species using the triphos ligand are cationic. The proposed mechanism was well confirmed by experimental as well as computational results. In order to further optimize this system to achieve a higher activity, this knowledge is of significant use because additives can strongly influence the catalyst. Also, the choice of solvent will play an important role, as shown by the lower activity with **D** as catalyst when using THF. Potential coordinating solvents may on the one hand have a negative effect on the active catalytic species

DOI: 10.1021/acs.organomet.5b00003
Organometallics XXXX, XXX, XXX−XXX

but could stabilize the cationic species and also improve the solvation of the ammonium salts on the other. It also has to be considered that when using toluene a water phase can be gradually formed during the reaction. This may have an influence on the activity when compared with that of THF, which is completely miscible with water. The different solubilities of NH_3 in THF and toluene also have to be taken into account regarding the activity of the catalytic system. In this context, it is still not clear which effect is the most relevant to explain the significant higher activity in toluene compared to that of the catalysis run in THF. Further investigations into how the triphos-ligand can be modified to improve the catalyst performance and on the role of different solvents in the catalytic system are ongoing.

EXPERIMENTAL SECTION

General Considerations. All manipulations were carried out under an anaerobic atmosphere of argon in a glovebox or using standard Schlenk line techniques. All nondeuterated solvents were dried using an MBraun SPS-800 solvent purification system and degassed prior to use, except for anhydrous pentane which was purchased and degassed prior to use. All reagents were purchased from Aldrich, except for [$(PPh_3)_3$Ru(H)(Cl)(CO)], which was purchased from Alfa Aesar. Liquid reagents were distilled prior to use, and all others were used without further purification. [(triphos)Ru(H)(Cl)(CO)] (**1**) was prepared by literature methods.[12] Dichloromethane-d_2 and THF-d_8 were dried over CaH_2 prior to distillation. ^{1}H, ^{2}H{^{1}H}, ^{13}C{^{1}H}, ^{31}P{^{1}H}, and ^{19}F{^{1}H} NMR spectra were recorded on a Bruker Avance 200 or 400 MHz spectrometer. ^{1}H and ^{13}C chemical shifts are reported relative to residual solvent signals of CD_2Cl_2 (5.32 and 54.0 ppm), THF-d_8 (5.38 and 67.21 ppm), and pyridine-d_5 (8.74 pp for ^{1}H). ^{31}P{^{1}H} chemical shifts are referenced to an external 85% solution of phosphoric acid, and ^{19}F{^{1}H} chemical shifts are referenced to external neat $CFCl_3$. The ^{13}C NMR data were assigned by HSQC and HMBC spectra. FAB and HR mass spectrometry was measured at the Mass Spectrometry Facility (Institute of the Organic Chemistry, University Heidelberg). Gas chromatography was performed on an Agilent 6890N modular GC base equipped with a split-mode capillary injection system and a flame ionization detector using a BGB-5 capillary column (Agilent 122−1033; 30 m × 0.32 mm × 0.25 μm; He flow 1.0 mL/min, program: initial 50 °C for 2 min, ramp 6 °C/min, 300 °C for 10 min). Starting materials and products had the following retention times: cyclohexanone (t_R = 10.49 min), octanal (t_R = 13.47 min), octylamine (t_R = 14.54 min), 1-octanol (t_R = 15.16 min), hexanitrile (t_R = 15.40 min), acetophenone (t_R = 15.60 min), dioctylamine (t_R = 31.34 min), 18crown6 (t_R = 34.79 min), and trioctylamine (t_R = 41.71 min). All in situ IR experiments were performed using a ReactIR 45m, purchased from Mettler Toledo with a titanium autoclave from Paar Instruments and an integrated ATR probe. Elemental analyses were performed in the "Mikroanalytisches Laboratorium der Chemischen Institute der Universität Heidelberg".

General Procedure for the Catalyst Tests Given in Table 1 and Monitoring Reactivity over Time of Catalyst System D and Complexes 1 and 2. To a Parr autoclave (160 mL, stainless steel V4A) equipped with a magnetically coupled inclined blade stirrer was added 0.14 mmol of catalyst (**D**: triphos (88 mg); $(PPh_3)_3$Ru(H)(Cl)(CO) (133 mg); **1** (111 mg); **2** (106 mg); and **3** (128 mg)), THF (30 mL) and 1-octanol (9.1 g, 50 mmol) under an inert argon atmosphere. The Parr autoclave was sealed, and NH_3 (7.2 g, 500 mmol) was introduced at room temperature as condensed liquid. The autoclave was heated to 155 °C for 24 h with vigorous stirring (200−500 rpm). A sample was removed periodically, and the product mixture was analyzed by GC (30 m RTX5-0.32 mm, 1,5 μm; 60-4-280/20), and the conversion of 1-octanol and the yield of 1-octylamine were calculated based on GC area%.

Synthesis of [(Triphos)Ru(H)$_2$(CO)] (2). A round-bottomed Schlenk flask (100 mL) was charged with [(triphos)RuHCl(CO)] (**1**, 980 mg, 1.2 mmol, 1 equiv) and THF (25 mL). A 1.0 M solution of $NaHBEt_3$ in THF (3.1 mL, 3.1 mmol, 2.5 equiv) was added dropwise. The white suspension was heated at reflux for 16 h to give a red solution. The solution was filtered to remove a small amount of white precipitate, and the solvent volume was reduced under vacuum to ∼5 mL. Pentane (40 mL) was slowly added to give [(triphos)Ru(H)$_2$(CO)] (**2**, 750 mg, 0.99 mmol, 83% yield) as a light yellow solid after filtration. All spectroscopic data are identical to those reported in the literature.[14]

General Procedure for NMR-Scale Conversion of [(Triphos)Ru(H)$_2$(CO)] (2) to [(Triphos)Ru(H)(X)(CO)] (1 and 3). A Teflon capped NMR tube was charged with [(triphos)Ru(H)$_2$(CO)] (**2**, 20 mg, 0.026 mmol, 1 equiv), [NH_4][Cl] (14 mg, 0.26, 10 equiv), or [NH_4][Br] (25 mg, 0.26, 10 equiv) and pyridine-d_5 (0.5 mL). The solution was mixed and placed in an oil bath at 110 °C and checked periodically by ^{31}P{^{1}H} and ^{2}H NMR spectroscopy.

(a) For [NH_4][Cl]: After 25 h, the ^{31}P{^{1}H} NMR spectrum showed mostly **1** (83%) with a small amount of **2** (7%) and several unidentified products (10%).

(b) For [NH_4][Br]: After 16 h, the ^{31}P{^{1}H} NMR spectrum showed mostly [(triphos)Ru(H)(Br)(CO)] (**5**, 82%) with several unidentified products (18%). ^{31}P{^{1}H} NMR (81.0 MHz, pyridine-d_5, δ): 50.6 (dd, $^2J_{PP}$ = 39 Hz, $^2J_{PP}$ = 17 Hz, 1P), 13.3 (dd, $^2J_{PP}$ = 39 Hz, $^2J_{PP}$ = 32 Hz, 1P), 0.7 (dd, $^2J_{PP}$ = 33 Hz, $^2J_{PP}$ = 17 Hz, 1P). ^{1}H NMR (200.2 MHz, pyridine-d_5, δ): 8.14−7.77 (m, 12H, Ph), 7.31−6.98 (m, 18H, Ph), 3.11−2.88 (m, 2H, CH_2P), 2.59−2.49 (m, 4H, CH_2P), 1.68 (s, 3H, CH_3), −5.73 (dt, $^2J_{HP}$ = 92 Hz, $^2J_{HP}$ = 17 Hz, 1H, RuH).

General Procedure for the Conversion of [(Triphos)Ru(H)(Cl)(CO)] (1) to [(Triphos)Ru(H)$_2$(CO)] (2) with Ammonia and Hydrogen. [(Triphos)Ru(H)(Cl)(CO)] (**1**, 50 mg, 0.063 mmol) and THF (20 mL) were added to two separate premex autoclaves (60 mL, stainless steel) equipped with a magnetically coupled propeller blade stirrer, under an inert argon atmosphere. One autoclave was charged with NH_3 (6 bar) and hydrogen gas (20 bar), while the other was charged with only hydrogen (20 bar). The autoclave was heated to 165 °C for 1.5 h with vigorous stirring (200−300 rpm). The autoclaves were vented, and the solution was added to a round-bottomed Schlenk flask (100 mL) in the glovebox. The solvent was removed under reduced pressure, the light yellow residue was partially dissolved in THF-d_8 (0.5 mL), and the composition was determined by ^{31}P{^{1}H} NMR spectroscopy.

(a) For NH_3 and H_2: The reaction mixture contained mostly [(triphos)Ru(H)$_2$(CO)] (**2**, 85%), a small amount of [(triphos)Ru(H)(Cl)(CO)] (**1**, 6%), and 1−2 unidentified products (9%).

(b) For H_2: In this case, the ^{31}P{^{1}H} NMR of the residue was also checked in CD_2Cl_2 due to the low solubility of **1** in THF. The reaction mixture contained [(triphos)Ru(H)(Cl)(CO)] (**1**, 67%), [(triphos)Ru(H)$_2$(CO)] (**2**, 27%), and 1−2 unidentified products (6%).

General Procedure for Catalyst Screening of 1 and 2 with Additives. To a premex autoclave (60 mL, stainless steel) equipped with a magnetically coupled propeller blade stirrer was added the catalyst (**1** (36 mg, 0.046 mmol); **2** (37 mg, 0.046 mmol)), toluene (17 mL), 1-octanol (3.0 g, 23 mmol), and the additive, under an inert argon atmosphere. The autoclave was sealed, and NH_3 (6 bar) was introduced at room temperature as a gas. The autoclave was heated to 165 °C for 15 h with vigorous stirring (200−300 rpm). A sample of the product mixture was analyzed by GC, and the conversion of 1-octanol and the yield of 1-octylamine were calculated based on GC area %.

(a) Catalyst **1**, no additive, and catalyst resting state determination: When cooled, the autoclave was vented and flushed with argon for 20 min. In a glovebox, the mixture was added to a round-bottomed Schlenk flask (100 mL), and the solvent was removed under vacuum. Pentane was added to the high boiling residue to give a yellow precipitate. The mixture was filtered, and the residue was dissolved in CD_2Cl_2. The ^{31}P{^{1}H} and ^{1}H NMR spectra showed [(triphos)Ru(H)$_2$(CO)] (**2**) as the only product. Product distribution: 1-octanol (37%), octylamine (52%), dioctylamine (6%), hexanenitrile (3%), and other (2%).

(b) Catalyst 1 + [NH_4][Cl]: additive, [NH_4][Cl] (25 mg, 0.46 mmol); product distribution, 1-octanol (33%), octylamine (54%),

DOI: 10.1021/acs.organomet.5b00003
Organometallics XXXX, XXX, XXX−XXX

dioctylamine (5%), trioctylamine (1%), hexanenitrile (6%), and other (1%).

(c) Catalyst **1** + octanal: additive, octanal (59 mg, 0.46 mmol); product distribution, 1-octanol (11%), octylamine (80%), dioctylamine (2%), trioctylamine (1%), hexanenitrile (3%), and other (3%).

(d) Catalyst **1** + NaCl and 18crown6: additive, NaCl (27 mg, 0.46 mmol) and 18crown6 (122 mg, 0.46 mmol); product distribution, 1-octanol (63%), octylamine (31%), trioctylamine (4%), and other (2%).

(e) Catalyst **1** + 18crown6: additive, 18crown6 (122 mg, 0.46 mmol); product distribution, 1-octanol (12%), octylamine (78%), dioctylamine (4%), trioctylamine (2%), hexanenitrile (2%), and other (2%).

(f) Catalyst **1** + 18crown6 and octanal: additive, 18crown6 (122 mg, 0.46 mmol), octanal (59 mg, 0.46 mmol); product distribution, 1-octanol (4%), octylamine (84%), dioctylamine (2%), trioctylamine (1%), hexanenitrile (2%), and other (7%).

(g) Catalyst **2**, no additive: product distribution, 1-octanol (75%), octylamine (17%), dioctylamine (1%), trioctylamine (1%), and other (6%).

(h) Catalyst **2** + $[NH_4][Cl]$, octanal, and H_2O: additive, $[NH_4][Cl]$ (25 mg, 0.46 mmol), octanal (59 mg, 0.46 mmol), and water (8.2 mg, 0.46 mmol); product distribution, 1-octanol (39%), octylamine (52%), trioctylamine (1%), hexanenitrile (6%), and other (2%).

(i) Catalyst **2** + $[NH_4][Cl]$ and octanal: additive, $[NH_4][Cl]$ (25 mg, 0.46 mmol) and octanal (59 mg, 0.46 mmol); product distribution, 1-octanol (13%), octylamine (60%), dioctylamine (11%), hexanenitrile (8%), and other (8%).

(j) Catalyst **2** + $[NH_4][Cl]$: additive, $[NH_4][Cl]$ (25 mg, 0.46 mmol); product distribution, 1-octanol (38%), octylamine (47%), dioctylamine (3%), hexanenitrile (6%), and other (6%).

(k) Catalyst **2** + octanal and H_2O: additive, octanal (59 mg, 0.46 mmol) and water (8.2 mg, 0.46 mmol); product distribution, 1-octanol (100%).

(l) Catalyst **2** + octanal, acetone, cyclohexanone, or acetophenone: additive, octanal (59 mg, 0.46 mmol), acetone (28 mg, 0.46 mmol), cyclohexanone (45 mg, 0.46 mmol), and acetophenone (55 mg, 0.46 mmol); product distribution, 1-octanol (100%).

(m) Catalyst **2** + cyanohydrin: additive, cyanohydrin (39 mg, 0.46 mmol); product distribution, 1-octanol (100%).

(n) Catalyst **2** + $[NH_4][F]$: additive, $[NH_4][F]$ (17 mg, 0.46 mmol); product distribution, 1-octanol (75%), octylamine (22%), trioctylamine (1%), and other (2%).

(o) Catalyst **2** + $[NH_4][Br]$: additive, $[NH_4][Br]$ (45 mg, 0.46 mmol); product distribution, 1-octanol (70%), octylamine (20%), dioctylamine (3%), trioctylamine (3%), and other (4%).

(p) Catalyst **2** + $[NH_4][I]$: additive, $[NH_4][I]$ (67 mg, 0.46 mmol); product distribution, 1-octanol (100%).

(q) Catalyst **2** + NaCl and 18crown6: additive, NaCl (27 mg, 0.46 mmol) and 18crown6 (122 mg, 0.46 mmol); product distribution, 1-octanol (100%).

In Situ Monitoring of 1 Catalyzed Alcohol Amination by IR Spectroscopy. Toluene (8 mL) was added to the ReactIR autoclave and heated to 80 °C. A suspension of [(triphos)Ru(H)(Cl)(CO)] (**1**, 111 mg, 0.13 mmol, 7 mol %) in toluene (2 mL), 1-octanol (3.0 mL, 19.0 mmol), and ammonia (6 bar) were sequentially added. A background IR spectrum was taken after each addition. The sample was then heated to 150 °C for 2 h and then to 160 °C for about 4 h. An IR spectrum was recorded every minute throughout the experiment.

■ ASSOCIATED CONTENT

Supporting Information

Computational details and alternative pathways S1, S2, and S3 as well as a text file of all computed molecule Cartesian coordinates in .xyz format for convenient visualization are given in the Supporting Information. The Supporting Information is available free of charge on the ACS Publications website at DOI: 10.1021/acs.organomet.5b00003.

■ AUTHOR INFORMATION

Corresponding Author

*E-mail: thomas.schaub@basf.com.

Notes

The authors declare no competing financial interest.

■ ACKNOWLEDGMENTS

We thank professor Gerard van Koten for his suggestion on possibly active species beyond the complexes observed during catalysis. M.H. thanks A. Schäfer for helpful discussions and P. Deglmann for highly valuable mechanistic suggestions. CaRLa (Catalysis Research Laboratory) is cofinanced by Ruprechts-Karls-Universtity Heidelberg (Heidelberg University) and BASF SE.

■ REFERENCES

(1) Eller, K.; Henkes, E.; Rossbacher, R.; Höke, H. *Ullmann's Encylopedia of Industrial Chemistry*; Wiley-VCH: Weinheim, Germany, 2012; Vol. 2, pp 647−698. DOI: 10.1002/14356007.a202_1.

(2) For selected reviews on homogenously catalyzed alcohol amination, see: (a) Gunanathan, C.; Milstein, D. *Science* **2013**, *341*, 122297121. (b) Kim, J.; Kim, H. J.; Chang, S. *Eur. J. Org. Chem.* **2013**, 3201−3213. (c) Klinkenberg, J. L.; Hartwig, J. F. *Angew. Chem., Int. Ed.* **2011**, *50*, 86−95. (d) Bähn, S.; Imm, S.; Neubert, L.; Zhang, M.; Neumann, H.; Beller, M. *ChemCatChem* **2011**, *3*, 1853−1864.

(3) Gunanathan, C.; Milstein, D. *Angew. Chem., Int. Ed.* **2008**, *47*, 8661−8664.

(4) Ye, X.; Plessow, P. N.; Brinks, M. K.; Schelwies, M.; Schaub, T.; Rominger, F.; Paciello, R.; Limbach, M.; Hofmann, P. *J. Am. Chem. Soc.* **2014**, *136*, 5923−5929.

(5) Imm, S.; Bähn, S.; Neubert, L.; Neumann, H.; Beller, M. *Angew. Chem., Int. Ed.* **2010**, *49*, 8126−8129.

(6) Pingen, D.; Müller, C.; Vogt, D. *Angew, Chem. Int. Ed.* **2010**, *49*, 8130−8133.

(7) (a) Imm, S.; Bähn, S.; Zhang, M.; Neubert, L.; Neumann, H.; Klasovsky, F.; Pfeffer, J.; Haas, T.; Beller, M. *Angew. Chem., Int. Ed.* **2011**, *50*, 7599−7603. (b) Schaub, T.; Buschhaus, B.; Brinks, M. K.; Schelwies, M.; Paciello, R.; Melder, J. P.; Merger, M. Method for producing primary amines by homogeneously catalyzed amination of alcohols. WO 2012/119927, 2012.

(8) Baumann, W.; Spannenberg, A.; Pfeffer, J.; Haas, T.; Köckritz, A.; Martin, A.; Deutsch, J. *Chem.—Eur. J.* **2013**, *19*, 17702−17706.

(9) (a) Walther, G.; Deutsch, J.; Martin, A.; Baumann, F. E.; Fridag, D.; Franke, R.; Köckritz, A. *ChemSusChem* **2011**, *4*, 1052−1054. (b) Pingen, D.; Diebolt, O.; Vogt, D. *ChemCatChem* **2013**, *5*, 2905−2912.

(10) Pingen, D.; Lutz, M.; Vogt, D. *Organometallics* **2014**, *33*, 1623−1629.

(11) Pingen, D.; Lebl, T.; Lutz, M.; Nicho, G. S.M; Kamer, P. C. J.; Vogt, D. *Organometalics* **2014**, *33*, 2798−2805.

(12) Sung, K.−M; Huh, S.; Jun, J.−M. *Polyhedron* **1999**, *18*, 469−479.

(13) Williams, D.; Fleming, I. *Spectroscopic Methods in Organic Chemistry*, 6th ed.; McGraw-Hill Education: Berkshire, U.K., 2008.

(14) Bakhmutov, V. I.; Bakhmutova, E. V.; Belkova, N. V.; Bianchini, C.; Epstein, L. M.; Masi, D.; Peruzzini, M.; Shubina, E. S.; Vorontsov, E. V.; Zanobini, F. *Can. J. Chem.* **2001**, *79*, 479−489.

(15) Eshuis, H.; Yarkony, J.; Furche, F. *J. Chem. Phys.* **2010**, *132*, 234114.

(16) Eshuis, H.; Bates, J. E.; Furche, F. *Theor. Chem. Acc.* **2012**, *131*, 1084.

(17) *TURBOMOLE V6.4 2012, a Development of University Karlsruhe and Forschungszentrum Karlsruhe GmbH, 1898−2007*, TURBOMOLE GmbH, since 2007; available from http://www.turbomole.com.

(18) Eckert, F.; Klamt, A. *COSMOtherm*, version C3.0, release 14.01; COSMOlogic GmbH & Co.: KG, Leverkusen, Germany, 2013.

DOI: 10.1021/acs.organomet.5b00003
Organometallics XXXX, XXX, XXX−XXX

(19) Chase, M. W.; Daives, C. A.; Downey, J. R.; Frurip, D. J.; McDonald, R. A.; Syverud, A. N. JANAF thermochemical tables. *J. Phys. Chem. Ref. Data* **1985**, *14*, Suppl. 1.
(20) Knacke, O., Kubaschewski, O., Hesselmann, K., Eds. *Thermochemical Properties of Inorganic Substances*, 2nd ed.; Springer: Heidelberg, Germany, 1991.
(21) Plessow, P. New Insights into Homogeneously Catalyzed Reactions: Theoretical Investigations. Ph.D. Thesis, University of Heidelberg, Heidelberg, Germany, 2014.
(22) Sieffert, N.; Récreux, R.; Lorusso, P.; Cole-Hamilton, D. J.; Bühl, M. *Chem.—Eur. J.* **2014**, *20*, 4141−4155.
(23) Hommeltoft, S. J.; Baird, M. C. *Organometallics* **1986**, *5*, 190−195.
(24) (a) Geilen, F. M. A.; Engendahl, B.; Hölscher, M.; Klankermayer, J.; Leitner, W. *J. Am. Chem. Soc.* **2011**, *133*, 14349−14358. (b) vom Stein, T.; Meuresch, M.; Limper, D.; Schmitz, M.; Hölscher, M.; Coetzee, J.; Cole-Hamilton, D. J.; Klankermayer, J.; Leitner, W. *J. Am. Chem. Soc.* **2014**, *136*, 13217−13225.
(25) (a) Rappert, T.; Yamamoto, A. *Organometallics* **1994**, *13*, 4984−4993. (b) Hara, Y.; Kusaka, H.; Inagaki, H.; Takahashi, K.; Wada, K. *J. Catal.* **2000**, *194*, 188−197.
(26) Savourey, S.; Lefèvre, G.; Berthet, J. C.; Thuéry, P.; Genre, C.; Cantat, T. *Angew. Chem., Int. Ed.* **2014**, *53*, 10466−10470.
(27) Buschmann, H.-J.; Schollmeyer, E. *Supramol. Sci.* **1998**, *5*, 139−142.

DOI: 10.1021/acs.organomet.5b00003
Organometallics XXXX, XXX, XXX−XXX